A Journal of the Gesellschaft Deutscher Chemiker

Angewandte International Edition

GDCh

Chemie

www.angewandte.org

Accepted Article

Title: Supramolecularly Assembled Nanocomposites as Biomimetic Chloroplasts for Enhancement of Photophosphorylation

Authors: Yue Li, Xiyun Feng, Anhe Wang, Yang Yang, Jinbo Fei, Bingbing Sun, Yi Jia, and Junbai Li

To be cited as: *Angew. Chem. Int. Ed.* 10.1002/anie.201812582
Angew. Chem. 10.1002/ange.201812582

Link to VoR: http://dx.doi.org/10.1002/anie.201812582
http://dx.doi.org/10.1002/ange.201812582

WILEY-VCH

10.1002/anie.201812582

WILEY-VCH

COMMUNICATION

Supramolecularly Assembled Nanocomposites as Biomimetic Chloroplasts for Enhancement of Photophosphorylation

Yue Li,[#a,b] Xiyun Feng,[#a,c] Anhe Wang,[#a,d] Yang Yang,[b] Jinbo Fei,[a] Bingbing Sun,[a,e] Yi Jia,[a] and Junbai Li*[a,e]

Abstract: Prototypes of natural biosystems provide new opportunities for artificial biomimetic systems to break the limits of natural reactions and achieve output control. However, mimicking unique natural structures and ingenious functions still remains a great challenge. Here, we have integrated multiple biochemical reactions into artificially designed compartments *via* molecular assembly. First, multicompartmental silica nanoparticles with hierarchical structures that mimic the chloroplasts were obtained by a templated synthesis. Then, photoacid generators and ATPase-liposomes were assembled inside and outside of silica compartments, respectively. Upon light illumination, protons produced by a photoacid generator in the confined space can drive the liposome-embedded enzyme ATPase towards ATP synthesis, which mimics the photophosphorylation process *in vitro*. The developed methodology enables fabrication of bioinspired nanoreactors for photobiocatalysis and provides insight for understanding sophisticated biochemical reactions.

Photophosphorylation reactions occurring in plant chloroplasts play an important role in the usage of solar energy, which has great potential as a clean, renewable and globally available energy source.[1] Chloroplasts are typically hierarchical organelles in which the light-harvesting pigments, electron transport chain, and enzymes are supramolecularly organized in typical stacking thylakoids, where light is captured then promote water splitting into oxygen, electrons and protons, and the produced proton gradients enable adenosine triphosphate (ATP) synthase to rotate and catalyze the synthesis of ATP and biomass to accomplish further energy conversion (Scheme 1).[2] However, limited by the natural energy conversion efficiency and the weak stability of natural photosystem complexes, many advanced artificial systems have been developed to enhance light harvesting or water splitting processes.[3] Other than this, the final solar-to-chemical energy conversion relies on the photophosphorylation efficiency due to the crucial function of ATP as an "energy currency".[2c] Notably, the rapid formation of a proton gradient and a membrane potential across the thylakoid membrane is the driving force for ATP production. Therefore, constructing a controllable mimicking chloroplast employing this strategy is of vital importance to enhance the final solar energy conversion efficiency. However, it still remains a great challenge to achieve large-scale production of ATP *in vitro* due to the sophisticated biocomponents coupled in the cascade reaction and the need for rapid formation of a proton gradient across the thylakoid membrane for enhanced ATP production.[4]

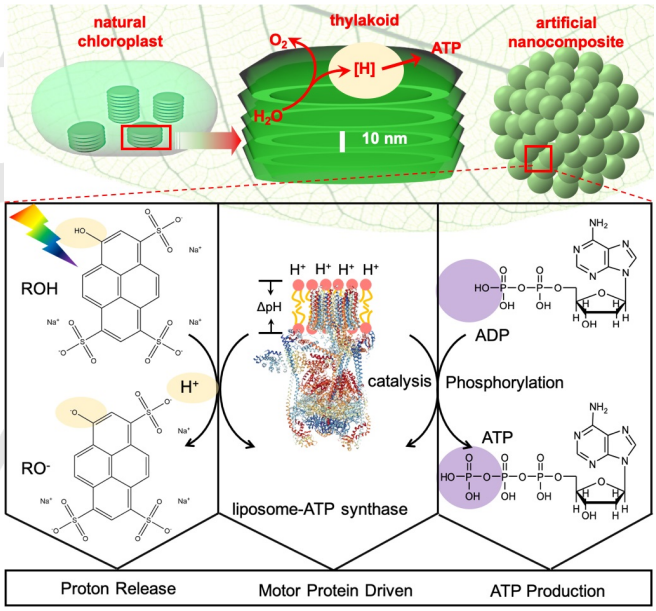

Scheme 1. Natural chloroplast multicompartment structures and biochemical reactions. A model of an artificially designed photophosphorylation system in synthesized nanocomposites.

As a spatially confined membrane protein, ATP synthase is anchored predominantly outside of the obstructed proton gradient in internal multicompartmental structures for efficient photophosphorylation.[5] Given the strong dependence on the dominant structure of multicompartment thylakoids, it's an urgent requirement to employ efficient light-sensitive pH-jump reagents as proton source[6] and integrate it with the protein motor with a mimicking strategy, through a more elegant method, supramolecular assembly.[7] Based on assembly, well-ordered and morphology-tunable reactors can be synthesized,[8] especially for biomimetic systems.[9] Among assembled systems, reactors at the nano and micro scales have attracted much attention because of their potential advantages for mass

[a] Dr. Y. Li, Dr. X. Feng, Dr. A. Wang, Dr. J. Fei, Dr. B. Sun, Dr. Y. Jia, Prof. Dr. J. Li
Beijing National Laboratory for Molecular Sciences (BNLMS), CAS Key Lab of Colloid, Interface and Chemical Thermodynamics, Institute of Chemistry, Chinese Academy of Sciences, Beijing, 100190, China.
E-mail: jbli@iccas.ac.cn
[b] Dr. Y. Li, Dr. Y. Yang
CAS Key Laboratory for Biomedical Effects of Nanomaterials and Nanosafety, National Center for Nanoscience and Technology, Beijing, 100190, China.
[c] Dr. X. Feng
Yunnan Normal University, Faculty of Chemistry and Chemical Engineering, Kunming, 650050, China.
[d] Dr. A. Wang
State Key Laboratory of Biochemical Engineering, Institute of Process Engineering, Chinese Academy of Sciences, Beijing, 100190, China.
[e] Dr. B. Sun, Prof. Dr. J. Li
University of Chinese Academic of Sciences, Beijing 100049, China.
[#] These authors contributed equally to this work.

Supporting information for this article is given via a link at the end of the document.

10.1002/anie.201812582

production *in vitro*.[10] As an extension, we have successfully constructed a spatially confined photophosphorylation nanoreactor through supramolecular assembly to mimic both the structures and the functions of natural chloroplasts. In detail, massive proton formation is achieved by photoacid being absorbed in the multicompartmental reaction room, and this approach is based on short laser pulses as optical "switches" introducing an instantaneous change in the pH value for the activation of protein function. Then, ATP synthase is reconstituted with liposomes and further stabilized on the surface of a silica nanoparticle. Hence, using mesoporous silica as a three-dimensional proton 'cage' and a lipid bilayer shell as a 'proton barrier', spatial control of the proton concentration in nanoscale is obtained, and the photostimulated photoacid generator produces a rapid pH jump and triggers rotation of ATP synthase to produce ATP (Scheme 1). By this procedure, the large-scale photophosphorylation reaction was achieved through construction of quantity controlled, spatially defined nanoreactors using a simple supramolecular assembly method.

The fabrication process of the nanoreactor is shown in Fig. 1a. Hierarchical silica nanoparticles, as both photoacid repositories and liposome upholders, were obtained through a templating method.[11] In brief, $CaCO_3$ nanoparticles were prepared as templates allowing SiO_2 to duplicate the hierarchical structure (Fig. 1b,c). After removing the template, multi-compartmental SiO_2 nanoparticles were fabricated, yielding a packed array of globular pores of tens of nanometers in diameter and 10-15 nm in wall thickness (Fig. 1d,e). Then, poly(allylamine hydrochloride) (PAH), (8-hydroxypyrene-1,3,6-trisulfonate trisodium salt) (HPTS) and reconstituted ATP synthase-liposome were assembled successively through electrostatic interaction, and a carrier for proton gradient building was formed.[12] As a result, the proteoliposome was successfully assembled onto the HPTS-incorporated SiO_2 nanoparticles(Fig. f-i). Additional data from energy-dispersive X-ray spectroscopy (EDX) mapping (Fig. 1j) were collected to investigate the location of the key elements Si, N, Na, and P, mainly originating from SiO_2, PAH, HPTS and liposome-ATP synthase, respectively.

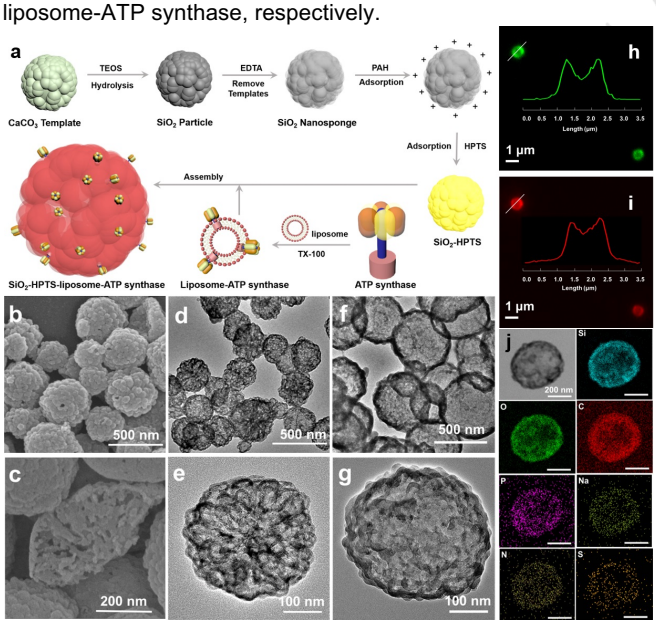

Figure 1. (**a**) The illustration of the biochemical reaction mechanism and the fabrication process: HPTS can be assembled into the multiple compartments of SiO_2 nanosponges by electrostatic interaction. With the coassembly of liposome-ATP synthase, light-mediated protons are generated and stored to form a proton gradient across the multicompartmental SiO_2 nanosponge for ATP production. (**b,c**) SEM images of hierarchical silica nanosponges. (**d,e**) TEM images of hierarchical silica nanosponges. (**f,g**) TEM images of SiO_2-HPTS@liposome-ATP synthase particles. (**h,i**) Fluorescence images of HPTS entrapped silica nanoparticles covered with Texas red-labeled liposome excited at 488 nm (green signal) and 561 nm (red signal), respectively. Insets are the green and red fluorescence signal distribution of two chosen particles in h and i, respectively. (**j**) EDX mapping of the individual SiO_2-HPTS@liposome-ATP synthase particle.

Assembled nanocomposites enable specific biochemistry reactions to be carried out in a confined space. In this case, the proton source is crucial for the integrated system. Photoacid generators are a class of proton-bearing small molecules that become acidic, lowering the pH value by several orders of magnitude, in the excited state and release their protons.[13] They have been used in several applications, including studies of chemical kinetics, where creating a rapid optical pH jump to initiate a proton-requiring process is desired.[14] HPTS was first used as a fluorescence pH indicator dye.[15] Its fluorescence in bulk water shows two distinct excitation bands corresponding to protonated (ROH) and deprotonated (RO^-) forms. When the pH in the bulk solution (pH_{bulk}) changed from 9.0 to 4.6, the intensities of the characteristic excitation bands at approximately 405 nm (ascribed to ROH) increased, and the band at approximately 458 nm (ascribed to RO^-) decreased (Fig. 2a), which is in good agreement with a previous report.[16] In dark, the pH value can be calculated by substituting the ratio I_{405}/I_{458} into the equation (inset of Fig. 2a).[16]

Other than its use as a fluorescence pH indicator, HPTS is also a well-known photoacid generator.[6b] It has a nearly neutral pKa (7.4) in its ground state, and this can be changed to a much lower value (pKa* 0.5) after photoexcitation.[17] In aqueous solution with a pH value larger than the pKa*, deprotonation of the photoacid occurs rapidly, and HPTS is converted into a strong acid by photolysis release of protons ($ROH \rightarrow RO^{-*}+H^+$) (Fig. 2b).[6b] Against this background, HPTS assembled in the nanocomposite was employed as a photoinduced proton source. However, when it is employed as a photoacid generator, the pH value cannot be calculated by a simple equation. The intensity peak has a slight blue shift, and the intensity of RO^- at 455 nm decreased with irradiation. After 18 min an excitation peak at 403 nm appeared (Fig. 2b). The disappearance of RO^- was due to the equilibrium between ROH and RO^- and the accumulated acidity was caused by the ROH-to-RO^{-*} transformation. After irradiation for a long period, it seems that the pH change is irreversible, and the jump of the pH value strongly depends on the time of stimulation. A large number of protons was then generated in the confined space of the nanoreactor (Fig. 2c).

10.1002/anie.201812582

WILEY-VCH

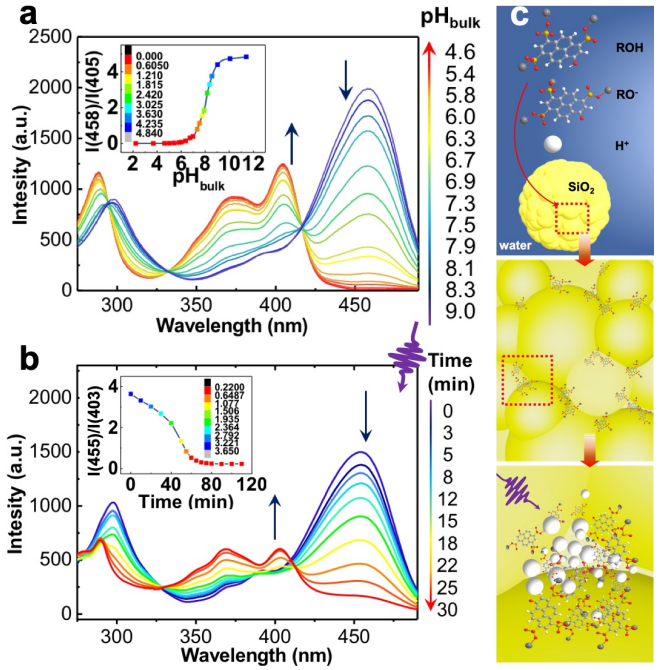

Figure 2. (**a**) Fluorescence excitation spectra (λ_{em}=513 nm) of HPTS in silica nanoparticles as a function of pH_{bulk}, and the inset is the pH-dependent value of Ex_{458}/Ex_{405}. The pH of the solution in a, b and c was adjusted using HCl and NaOH. (**b**) Time-dependent excitation spectra of SiO_2-HPTS in solution under white illumination, and the inset is the time-dependent value of Ex_{455}/Ex_{403} under illumination. To maintain the appropriate ionic strength, 100 mM NaCl was used. (**c**) Graphic illustration of spatially confined SiO_2-HPTS.

ATP synthase was isolated, reconstituted into liposome to form liposome-ATP synthase through a published procedure with minor modifications,[12b,16] then located on the surface of SiO_2-HPTS nanoparticle (Fig. 1f-j). To detect the proton gradient within the assembled nanoreactor, three different particles, SiO_2-HPTS, SiO_2-HPTS@liposome, and SiO_2-HPTS@liposome-ATP synthase, were investigated in the test solution. As a result, the pH_{bulk} rapidly decreased without liposome cover (dotted line), indicating that the protons freely diffused in the aqueous solution without the protection of liposomes (Fig. 3d). For SiO_2-HPTS@liposome the pH_{bulk} decreased much more slowly during the initial 30 min due to the protection of liposomes (solid line). However, the pH_{bulk} distinctly decreased with increasing time of light irradiation after 30 min, indicating leakage of protons. Furthermore, SiO_2-HPTS@liposome-ATP synthase was introduced to prove the function of the proton pump for comparison. It is obvious that SiO_2-HPTS@liposome-ATP synthase (dashed line) exhibited a higher proton throughput ability than did SiO_2-HPTS@liposome. The different values are shown in Fig. 3d (below). It was concluded that ATP synthase acted as a proton pump in the system mainly during the initial 30 min. Compared with the outside bulk solution, the localized acidification inside the core undergoes a significant pH change upon irradiation. The obtained protons generate a proton gradient that significantly affects the biochemical activity of transmembrane proteins. This cascade biocatalytic process can be clearly observed via the ATP synthase membrane channels converting the pH gradient into chemical energy, that is, ATP generation.[16]

Under light illumination, the outward pumping of protons generated by HPTS provides a driving force for ATP synthase rotary catalysis, synthesizing ATP detected by luciferin-luciferase bioluminescence assay.[12b,16] It is clearly seen that the ATP production continuously increased with increasing irradiation time within the first 70 min under illumination and reached a plateau after 70 min (Fig. 3a,b). Remarkably, the ATP production and the degree of pH decrease both occurred in response to the illumination intensity and HPTS amount. In the optical situation depicted in Fig. 3a,b, the samples containing 0.16 mM HPTS under 100 mW cm^{-2} light power could generate over 6 μmol ATP per mg ATP synthase within 122 min. In this case, during the first 10 s, the ATP production increased to 0.06586 μmol per mg ATP synthase s^{-1}. During this time, the average rate was 37.5402 ATP s^{-1} ATP $synthase^{-1}$ (Fig. 3c left), which represents the CF_oF_1-ATPase turnover frequency (TOF), and can be compared with the existing ATP production systems (Table S1). Moreover, the maximum rate (initial 10 s) of ATP production is associated with the light power and HPTS concentration, indicating that the generation rate can be precisely controlled (Fig. 3c). It is worth mentioning that higher values could be obtained if more particles were employed. In addition, Fig. 3f demonstrates that ATP synthesis could be simply triggered by light. These results further demonstrate that it is the light-induced local acidification that leads to activation of ATP synthase and delivers the chemiosmotic energy. Under illumination, the proton concentration gradient is built up, and the embedded ATP synthase can be switched on.

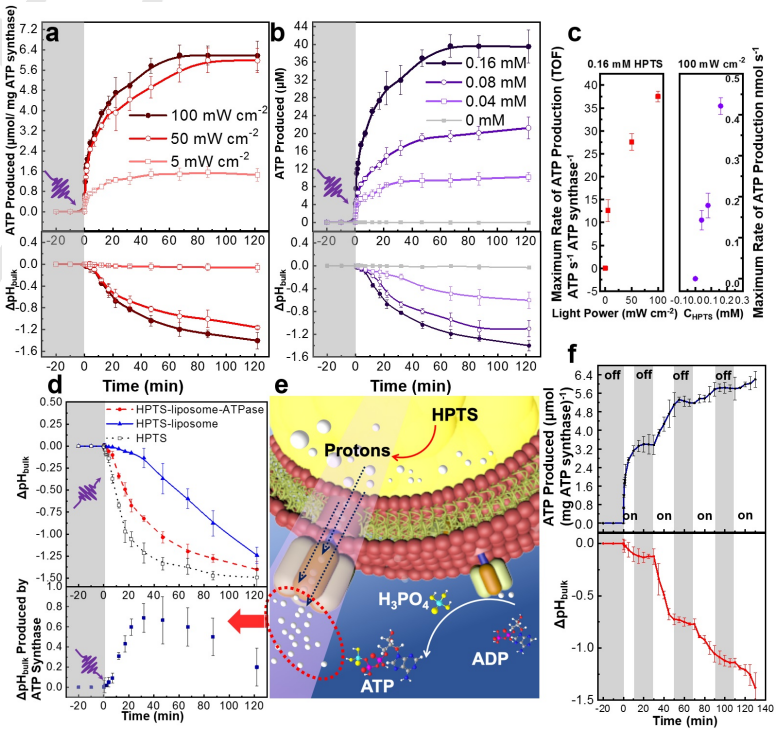

Figure 3. (**a**) Effect of different light power on ATP production and pH_{bulk} changes. (**b**) Effect of different HPTS concentrations on ATP production (μM) and pH_{bulk} changes. (**c**) Plots of maximum rate of ATP production vs. light power or HPTS concentration. (**d**,**e**) Light-dependent pH_{bulk} changes of different solutions containing HPTS (dotted line), HPTS-liposome (solid line) or HPTS-liposome-ATP synthase (dashed line) under illumination, and changes of the value of the solid line and the dashed line during time of illumination (below). (**f**) Light-triggered ATP synthesis and pH_{bulk} change of the SiO_2-HPTS-liposome-ATP synthase system through on/off cycles of light. All error bars refer to the standard deviation (n=3).

Overall, we have developed a facile and efficient strategy to mimic chloroplasts at the structural and functional levels in a nanocomposite system that involves photophosphorylation, mimicking the massive ATP production *in vitro*. In particular, a light switch and a pH jump trigger are combined in a coupling system to obtain a sophisticated cascade reaction through molecular assembly. Moreover, taking into account that there are many important chemical reactions and biological processes that depend on precise control, this method may provide a novel supramolecular assembly procedure to construct other biomimetic nanosystems with creative applications for remote control of biochemical synthesis and enzyme catalysis and, further, for stimuli-responsive drug delivery.

Experimental Section

Experimental details are shown in the Supporting Information.

Acknowledgements

The authors declare no competing interests.

The authors gratefully acknowledge the financial support for this research by the National Natural Science Foundation of China (No. 21433010, 21320102004, 21573248 and 21872151).

Keywords: supramolecular assembly • nanocomposite • photophosphorylation • organic-inorganic hybrid composites • nanostructures

[1] a) A. Hahn, J. Vonck, D. J. Mills, T. Meier, W. Kühlbrandt, *Science* **2018**, *360*, eaat4318, b) K. Y. Lee, S.-J. Park, K. A. Lee, S.-H. Kim, H. Kim, Y. Meroz, L. Mahadevan, K.-H. Jung, T. K. Ahn, K. K. Parker, K. Shin, *Nat. Biotechnol.* **2018**, *36*, 530-535.

[2] a) B. Daum, D. Nicastro, J. A. II, J. R. McIntosh, W. Kuhlbrandt, *Plant Cell* **2010**, *22*, 1299-1312; b) N. Nelson, C. F. Yocum, *Annu. Rev. Plant Biol.* **2006**, *57*, 521-565; c) N. Soga, K. Kimura, K. Kinosita, M. Yoshida, T. Suzuki, *Proc. Natl. Acad. Sci. U. S. A.* **2017**, *114*, 4960-4965.

[3]. a) K. Liu, R. R. Xing, Y. X. Li, Q. L. Zou, H. Möhwald, X. H. Yan, *Angew. Chem. Int. Ed.* **2016**, *55*, 12503-12507; b) Y. X. Wang, S. L. Li, L. B. Liu, F. T. Lv, S. Wang, *Angew. Chem. Int. Ed.* **2017**, *56*, 5308-5311; c) K. Liu, C. Q. Yuan, Q. L. Zou, Z. C. Xie, X. H. Yan, *Angew. Chem. Int. Ed.* **2017**, *56*, 7876-7880; d) W. Y. Wang, J. Chen, C. Li, W. M. Tian, *Nat. Commun.* **2014**, *5*, 8.

[4]. G. Steinberg-Yfrach, J. L. Rigaud, E. N. Durantini, A. L. Moore, D. Gust, T. A. Moore, *Nature* **1998**, *392*, 479-482.

[5] M. Forgac, *Nat. Rev. Mol. Cell Biol.* **2007**, *8*, 917-929.

[6] a) S. Bhosale, A. L. Sisson, P. Talukdar, A. Furstenberg, N. Banerji, E. Vauthey, G. Bollot, J. Mareda, C. Roger, F. Wüthner, N. Sakai, S. Matile, *Science* **2006**, *313*, 84-86; b) S. Kohse, A. Neubauer, A. Pazidis, S. Lochbrunner, U. Kragl, *J. Am. Chem. Soc.* **2013**, *135*, 9407-9411.

[7] a) J. M. Lehn, *Science* **1993**, *260*, 1762-1763; b) J. M. Lehn, *Science* **2002**, *295*, 2400-2403; c) J. F. Lutz, J. M. Lehn, E. W. Meijer, K. Matyjaszewski, *Nat. Rev. Mater.* **2016**, *1*, 14.

[8] a) E. S. Andersen, M. Dong, M. M. Nielsen, K. Jahn, R. Subramani, W. Mamdouh, M. M. Golas, B. Sander, H. Stark, C. L. P. Oliveira, J. S. Pedersen, V. Birkedal, F. Besenbacher, K. V. Gothelf, J. Kjems, *Nature* **2009**, *459*, 73-75; b) G. Decher, *Science* **1997**, *277*, 1232-1237; c) M. Eckle, G. Decher, *Nano Lett.* **2001**, *1*, 45-49; d) L. Tauk, A. P. Schroder, G. Decher, N. Giuseppone, *Nat. Chem.* **2009**, *1*, 649-656; e) M. P. Pileni, *Nat. Mater.* **2003**, *2*, 145-150; f) H. He, B. Xu, *Bull. Chem. Soc. Jpn.* **2018**, *91*, 900-906.

[9] a) K. Ariga, Q. M. Ji, T. Mori, M. Naito, Y. Yamauchi, H. Abe, J. P. Hill, *Chem. Soc. Rev.* **2013**, *42*, 6322-6345; b) X. Zheng, G. Shen, C. Wang, Y. Li, D. Dunphy, T. Hasan, C. J. Brinker, B.-L. Su, *Nat. Commun.* **2017**, *8*, 1492; c) Z. Y. Tang, Y. Wang, P. Podsiadlo, N. A. Kotov, *Adv. Mater.* **2006**, *18*, 3203-3224; d) M. J. Harrington, A. Masic, N. Holten-Andersen, J. H. Waite, P. Fratzl, *Science* **2010**, *328*, 216-220; e) X. Gao, L. Jiang, *Nature* **2004**, *432*, 36; f) F. Pu, J. Ren, X. Qu, *Chem. Soc. Rev.* **2018**, *47*, 1285-1306.

[10] a) T. G. Shutava, D. S. Kommireddy, Y. M. Lvov, *ACS Nano* **2009**, *3*, 1877-1885; b) K. Ariga, T. Mori, J. P. Hill, *Adv. Mater.* **2012**, *24*, 158-176; c) H. Gustafsson, K. Holmberg, *Adv. Colloid Interface Sci.* **2017**, *247*, 426-434; d) T. G. Shutava, D. S. Kommireddy, Y. M. Lvov, *J. Am. Chem. Soc.* **2006**, *128*, 9926-9934; e) K. T. Kim, J. Cornelissen, R. J. M. Nolte, J. C. M. van Hest, *Adv. Mater.* **2009**, *21*, 2787-2797; f) M. Yang, H. Chan, G. Zhao, J. H. Bahng, P. Zhang, P. Král, N. A. Kotov, *Nat. Chem.* **2017**, *9*, 287-294; g) W. C. Feng, J. Y. Kim, X. Z. Wang, H. A. Calcaterra, Z. B. Qu, L. Meshi, N. A. Kotov, *Sci. Adv.* **2017**, *3*, 12; h) B. Yeom, T. Sain, N. Lacevic, D. Bukharina, S. H. Cha, A. M. Waas, E. M. Arruda, N. A. Kotov, *Nature* **2017**, *543*, 95-99; i) R. K. Soong, G. D. Bachand, H. P. Neves, A. G. Olkhovets, H. G. Craighead, C. D. Montemagno, *Science* **2000**, *290*, 1555-1558; j) M. Komiyama, K. Yoshimoto, M. Sisido, K. Ariga, *Bull. Chem. Soc. Jpn.* **2017**, *90*, 967-1004; k) K. Ariga, D. T. Leong, T. Mori, *Adv. Funct. Mater.* **2018**, 28, 1702905.

[11] Y. J. Wu, Z. G. Wu, X. K. Lin, Q. He, J. B. Li, *ACS Nano* **2012**, *6*, 10910-10916.

[12] a) G. Schneider, G. Decher, N. Nerambourg, R. Praho, M. H. V. Werts, M. Blanchard-Desce, *Nano Lett.* **2006**, *6*, 530-536; b) L. Duan, Q. He, K. W. Wang, X. H. Yan, Y. Cui, H. Möhwald, J. B. Li, *Angew. Chem. Int. Ed.* **2007**, *46*, 6996-7000.

[13] M. Irie, *J. Am. Chem. Soc.* **1983**, *105*, 2078-2079.

[14] G. Zhao, T. Wang, *Angew. Chem. Int. Ed.* **2018**, *21*, 6120-6124.

[15] M. Rini, B. Z. Magnes, E. Pines, E. T. J. Nibbering, *Science* **2003**, *301*, 349-352.

[16] W. Qi, L. Duan, K. W. Wang, X. H. Yan, Y. Citi, Q. He, J. B. Li, *Adv. Mater.* **2008**, *20*, 601-603.

[17] M. Sedgwick, R. L. Cole, C. D. Rithner, D. C. Crans, N. E. Levinger, *J. Am. Chem. Soc.* **2012**, *134*, 11904-11907.

10.1002/anie.201812582

WILEY-VCH

COMMUNICATION

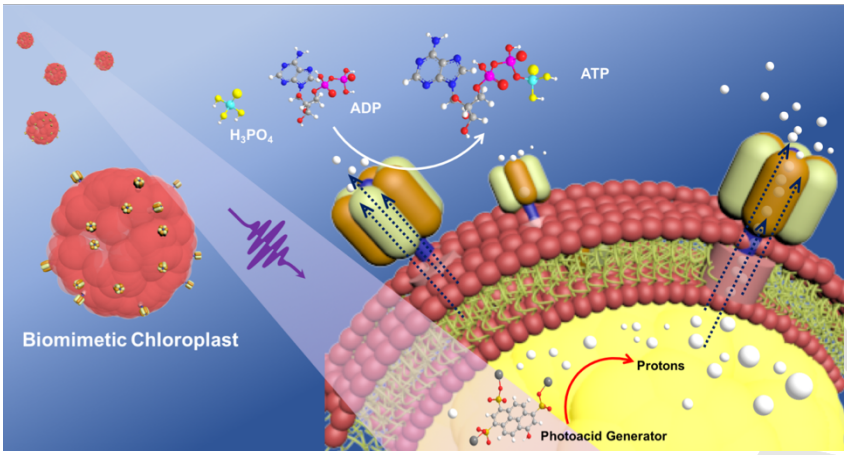

*Yue Li[#], Xiyun Feng[#], Anhe Wang[#], Yang Yang, Jinbo Fei, Bingbing Sun, Yi Jia, Junbai Li**

Page No. – Page No.

Supramolecularly Assembled Nanocomposites as Biomimetic Chloroplasts for Enhancement of Photophosphorylation

Table of Content:
Inspired by natural chloroplast compartment structures, hierarchical SiO_2 nanosponges are artificially designed, co-assembled with photoacid molecules and liposome-ATP synthase to form organic-inorganic hybrid nanocomposites for photophosphorylation output control achievement.